Asian Journal of Chemistry; Vol. 38, No. 6 (2026), 1581-1588
ASIAN JOURNAL OF CHEMISTRY
https://doi.org/10.14233/ajchem.2026.35714

# Multifunctional β-CD Ag/Cu Nanocomposite with Spongy Cotton Bud-Like Architecture for Photocatalytic and Biological Applications

M. SUBBULAKSHMI[1], K. LEELADEVI[2], T. KAVITHA[1,*] and P. SAROJINI[1]

[1]Department of Chemistry, Sri S. Ramasamy Naidu Memorial College (Affiliated to Madurai Kamaraj University), Sattur-626203, India
[2]Department of Chemistry, Ramco Institute of Technology, Rajapalayam-626117, India

*Corresponding author: E-mail: tkavitha@srnmcollege.ac.in

*Received*: 6 February 2026 *Accepted*: 14 May 2026 *Published online*: 31 May 2026 AJC-22385

Photocatalytic degradation of dyes using metal oxides and their composites is an effective method for the removal of pollutants from wastewater systems. Metal oxides exhibit enhanced efficiency due to their broad light absorption, rapid charge transfer dynamics and inherent p-n properties. In this work, a β-cyclodextrin-supported silver/copper nanocomposite (β-CD Ag/Cu) was successfully synthesised *via* a eco-friendly hydrothermal method using ascorbic acid as a reducing agent. The synthesized nanocomposite was characterized by XRD, SEM, EDAX and DRS-UV analyses, confirming its crystalline nature, unique spongy cotton bud-like morphology and an average particle size of ~110 nm. Optical studies revealed a narrow band gap of 1.95 eV, indicating efficient visible-light absorption. The β-CD Ag/Cu nanocomposite exhibited excellent photocatalytic activity towards methylene blue (MB) and methyl orange (MO) dyes, achieving degradation efficiencies of 86.20 and 95.71%, respectively. The effects of catalyst dosage, dye concentration and pH were systematically optimized. Furthermore, the nanocomposite demonstrated significant antioxidant activity against DPPH radicals and strong antibacterial activity against *Enterobacter* sp., *Pseudomonas* sp. and *Klebsiella* sp., with *Enterobacter* sp. showing the highest sensitivity (24 mm zone of inhibition).

**Keywords: β-Cyclodextrin, Host-guest interaction, Dye removal, Wastewater treatment.**

## INTRODUCTION

The photocatalytic method is regarded as a more environmentally friendly method since it promotes the use of a variety of materials, their high performance and their ability to convert solar energy to chemical energy [1-3]. The demand for industrialisation and its improvement has intensified in recent years due to the rapid growth of population. Along with being crucial for human growth, industry increases water pollution levels through its effluents by releasing inorganic and organic pollutants, heavy metal ions, dyes, antibiotics and other contaminants that have a negative impact on the environment. Dye pollution of surface and groundwater contributes significantly and it has severely detrimental consequences on living things [4]. Various methods such as precipitation, coagulation, adsorption, membrane filtration and flocculation have been employed for the removal of dyes from water [5]. Among these approaches, photocatalysis is considered one of the most effective techniques for the treatment of dye-contaminated wastewater [6-8].

Coupling of semiconductor oxides has been widely reported to reduce band gap energy, suppress electron-hole recombination and enhance photocatalytic activity. Several heterostructured systems including $WO_3$-$TiO_2$, $SnO_2$-ZnO, CuO-$TiO_2$, ZnO-$TiO_2$ and ZnO/CuO, have demonstrated improved photocatalytic efficiency [9-12]. Among these, CuO is a p-type semiconductor with a narrow band gap of 1.7 eV, exhibiting excellent optical and electrical properties along with low toxicity. Its combination with n-type semiconductors such as AgO extends light absorption into both UV and visible regions, making such composites highly effective for the degradation of organic pollutants.

Cyclodextrins (CDs), particularly β-cyclodextrin (β-CD), have attracted considerable attention due to their unique structural and physico-chemical properties, β-CD consists of seven glycosyl units linked through α-(1→4) bonds and possesses a hydrophobic inner cavity with multiple hydroxyl groups on the outer surface. The abundant hydroxyl groups enhance adsorption capability towards pollutants and facilitate the immobilization of metal oxides. Moreover, incor-

poration of β-CD into metal oxide systems improves visible-light absorption, reduces dye aggregation on catalyst surfaces and promotes efficient photocatalytic degradation by modifying surface morphology and increasing active surface interactions [13-16].

In the present work, a spongy cotton bud-like β-CD Ag/Cu nanocomposite with cork ball-like morphology was successfully fabricated for visible light-driven photocatalytic degradation of organic pollutants. β-CD acted as both stabilizing and reducing host matrix, improving charge transfer and minimizing electron–hole recombination through its electron-donating and hole-capturing properties. The synthesised nanocomposite was characterized using DRS UV-Vis, XRD, SEM and EDX analyses. The photocatalytic performance of β-CD Ag/Cu was evaluated towards the degradation of methylene blue (MB) and methyl orange (MO) dyes, where enhanced degradation efficiency was observed due to improved catalyst–dye interactions. In addition, the synthesised nanocomposite was further investigated for its antioxidant and antimicrobial activities, demonstrating its multi-functional application potential.

## EXPERIMENTAL

The chemicals viz. ascorbic acid, copper sulphate pentahydrate, silver nitrate and β-cyclodextrin (β-CD) were procured from Sigma-Aldrich, USA and used as received without further purification. All aqueous solutions required for the experimental studies were prepared using double-distilled water.

**Green synthesis of β-CD-Ag/Cu:** Initially, separate aqueous solutions of ascorbic acid (4.58 g in 20 mL distilled water), $CuSO_4 \cdot 5H_2O$, silver nitrate and β-CD (1.021 g in 20 mL distilled water) were prepared. The prepared solutions were mixed under continuous magnetic stirring and maintained at 80 ºC for 5 h. The resulting reaction mixture was then transferred into a 100 mL Teflon-lined autoclave and heated at 120 ºC for 4 h under hydrothermal conditions. The obtained precipitate was washed repeatedly with distilled water (four times) and absolute ethanol (once) to remove unreacted impurities. The purified product was dried at 110 ºC and subsequently calcined at 550 ºC for 5 h to obtain the β-CD Ag/Cu nanocomposite.

**Characterisation:** The crystalline structure of the synthesized β-CD Ag/Cu nanocomposite was analysed using a Bruker D2 X-ray diffractometer operated at 40 kV and 25 mA with Cu*K*α radiation (λ = 1.5406 Å). The diffraction patterns were recorded over a 2θ range of 5º-80º at a scanning rate of 0.02º. The optical properties and formation of the β-CD Ag/Cu nanocomposite were examined using a Shimadzu UV-2400 UV-visible spectrophotometer in the wavelength range of 200-800 nm. Surface morphology and structural features of the synthesized nanocomposite were investigated using a Carl Zeiss EVO 18 scanning electron microscope (SEM).

**Photocatalytic activity:** The photocatalytic activity of the β-CD Ag/Cu nanocomposite was evaluated through the degradation of methylene blue (MB) and methyl orange (MO) dyes under visible light irradiation using a 250 W xenon lamp. For the experiment, 100 mL dye solutions of desired concentration were mixed with the optimized amount of β-CD Ag/Cu catalyst. Prior to light irradiation, the suspension was magnetically stirred in dark conditions for 30 min to establish adsorption–desorption equilibrium between the dye molecules and catalyst surface. Subsequently, the reaction mixture was exposed to visible light irradiation. At regular intervals of 10 min, 6 mL aliquots were withdrawn and centrifuged to remove suspended catalyst particles. The residual dye concentration in the supernatant was analysed using a UV-visible spectrophotometer.

### Antimicrobial activity

**Microbial culture:** Three distinct bacterial strains, including *Enterobacter* sp., *Pseudomonas* sp. and *Klebsiella* sp., were employed in this investigation. All microbial isolates were identified and characterized through morphological, physiological and conventional biochemical tests in accordance with CLSI guidelines [17].

**Antimicrobial assay:** Using Muller-Hinton Agar plates and agar well diffusion on β-CD Ag/Cu nanocomposite, an antibacterial experiment was conducted. The test organisms were inoculated into nutrient broth and incubated overnight at 37 ºC to obtain a final inoculum concentration of $1.5 \times 10^8$ CFU/mL, corresponding to 0.5 McFarland turbidity standard. Using the standard microbial culture broth, MHA plates were grown. Dimethyl formamide (DMF) was used as solvent to prepare a β-CD Ag/Cu nanocomposite suspension at a concentration of 50 mg/mL. The antibacterial activity was evaluated using the agar well diffusion method. Wells of 6 mm diameter were aseptically prepared in Mueller-Hinton agar plates using a sterile cork borer. Different concentrations of the β-CD Ag/Cu nanocomposite (50, 75 and 100 μL) were introduced into the respective wells, while DMF served as the control. The plates were allowed to stand at room temperature for 30 min to facilitate diffusion and were subsequently incubated at 37 ºC for 18-24 h. After incubation, antibacterial activity was assessed by measuring the diameter of the clear zone of inhibition (ZOI) formed around each well, expressed in millimetres (mm).

**Antioxidant activity:** The antioxidant activity of the synthesised β-CD Ag/Cu nanocomposite was evaluated using the DPPH free radical scavenging assay, a rapid and reliable method for assessing antioxidant potential. DPPH exhibits a characteristic maximum absorbance at 517 nm, which decreases in the presence of antioxidant compounds due to free radical scavenging activity. In this study, 1 mL of ethanolic DPPH solution (25 mg/mL) was mixed with different concentrations of the β-CD Ag/Cu nanocomposite (12.5, 25, 37.5 and 50 μM). The reaction mixtures were shaken for 30 sec and incubated in dark conditions for 15 min at room temperature. The absorbance was then measured using a UV-Vis spectrophotometer at 517 nm. A significant decrease in absorbance indicated effective antioxidant activity of the β-CD Ag/Cu nanocomposite. The percentage inhibition of DPPH radicals was calculated using the following equation:

$$\text{DPPH inhibition (\%)} = \frac{A(b) - A(s)}{A(b)} \times 100 \qquad (1)$$

where A(b) = absorption of DPPH with ethanol alone (blank solution); A(s) = absorption of DPPH with nanocomposite with different concentrations.

## RESULTS AND DISCUSSION

**XRD spectra:** Fig. 1 illustrates the XRD pattern of the β-CD Ag/Cu nanocomposite synthesized through the hydrothermal method. The presence of sharp and well-defined diffraction peaks confirms the crystalline nature of the synthesised nanocomposite. The average crystallite size was estimated using the Scherrer equation, which correlates particle diameter (D) with the full width at half maximum (FWHM) of the diffraction peaks (λ = 0.154 nm). The calculated average crystallite size of the β-CD Ag/Cu nanocomposite was found to be approximately 110 nm.

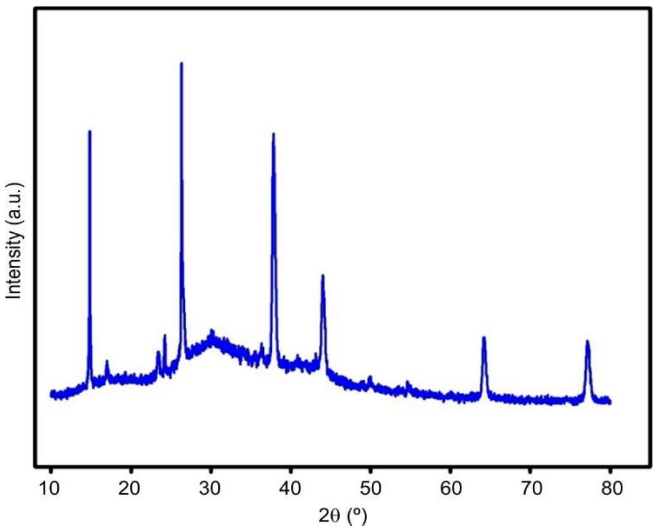


Fig. 1. XRD pattern of β-CD Ag/Cu nanocomposite

**Morphological studies:** Fig. 2a-d presents the SEM images of the synthesised β-CD Ag/Cu nanocomposite, illustrating its surface morphology and structural features. The SEM micrographs reveal the formation of unique spongy cotton bud-like Cu structures dispersed over Ag cork ball-like particles. The three-dimensional morphology of the nanocomposite (Fig. 2d) exhibited particle sizes ranging from 105.6 to 363.5 nm with nearly spherical architecture. The β-CD matrix supported the distribution of these spongy Cu nanostructures on the Ag surfaces, resulting in aggregated particle assemblies [18]. A slight degree of nanoparticle agglomeration and uneven surface morphology was also observed, possibly due to the presence of the capping agent. Furthermore, the particles were found to be non-uniformly distributed throughout the β-cyclodextrin matrix [19].

**EDAX microanalysis:** Fig. 3 illustrates the area-specific EDAX analysis of the synthesized β-CD Ag/Cu nanocomposite. The EDAX spectrum confirmed the presence of the constituent elements, comprising 39.4 wt.% silver, 30.7 wt.% carbon, 27.6 wt.% oxygen and 2.3 wt.% copper. Furthermore, elemental mapping analysis demonstrated the distribution of Ag, Cu, C and O elements throughout the β-CD Ag/Cu nanocomposite matrix (Fig. 4).

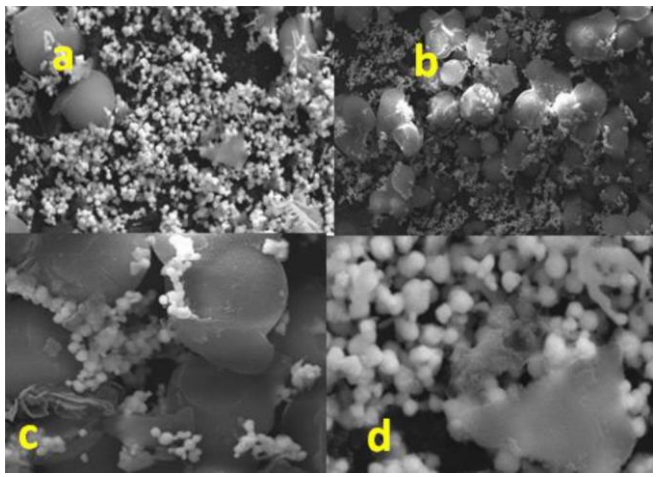


Fig. 2. SEM images of β-CD Ag/Cu

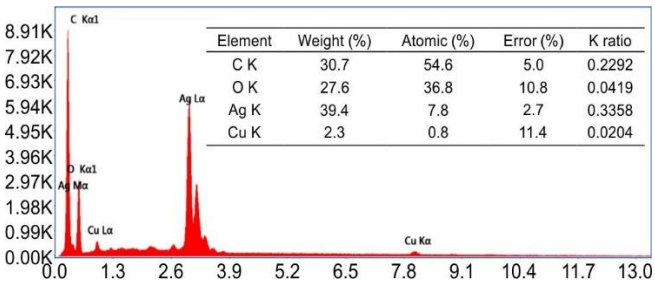


Fig. 3. EDX spectrum of β-CD Ag/Cu

**Optical studies:** DRS-UV spectroscopy was employed to investigate the optical properties and visible-light absorption behaviour of the β-CD Ag/Cu nanocomposite, as shown in Fig. 5, while the corresponding band gap values are presented in Fig. 5b. A noticeable colour change in the β-CD Ag/Cu suspension further indicated the formation of the nanocomposite. The diffuse reflectance UV-visible spectra were recorded in the wavelength range of 300-700 nm to analyse the optical response and energy band structure of the synthesised material [20]. The optical band gap energy of the β-CD Ag/Cu nanocomposite was determined using Tauc's plot equation [21]:

$$\alpha h\nu = A\,(E_g - h\nu)^2 \qquad (2)$$

where α is the absorption coefficient; hν is light energy; A is proportionality constant and $E_g$ is band gap. The β-CD Ag/Cu nanocomposite exhibited a band gap energy of 1.95 eV with an absorption edge at 450 nm in the visible region.

**Photocatalytic activity of β-CD Ag/Cu towards MB and MO dyes:** The photocatalytic activity of the synthesized β-CD Ag/Cu nanocomposite was evaluated through the visible light-induced degradation of methylene blue (MB) and methyl orange (MO) dyes (Fig. 6a-b). The degradation process was monitored using UV-visible spectroscopy at 653 nm for MB and 464 nm for MO. The nanocomposite achieved degradation efficiencies of 86.20% for MB within 110 min and 95.71% for MO within 60 min. The enhanced photocatalytic performance may be attributed to the reduced recombination of photogenerated electron–hole pairs [22-24].

**Different dosage and concentration:** Optimization of experimental parameters such as catalyst loading and dye

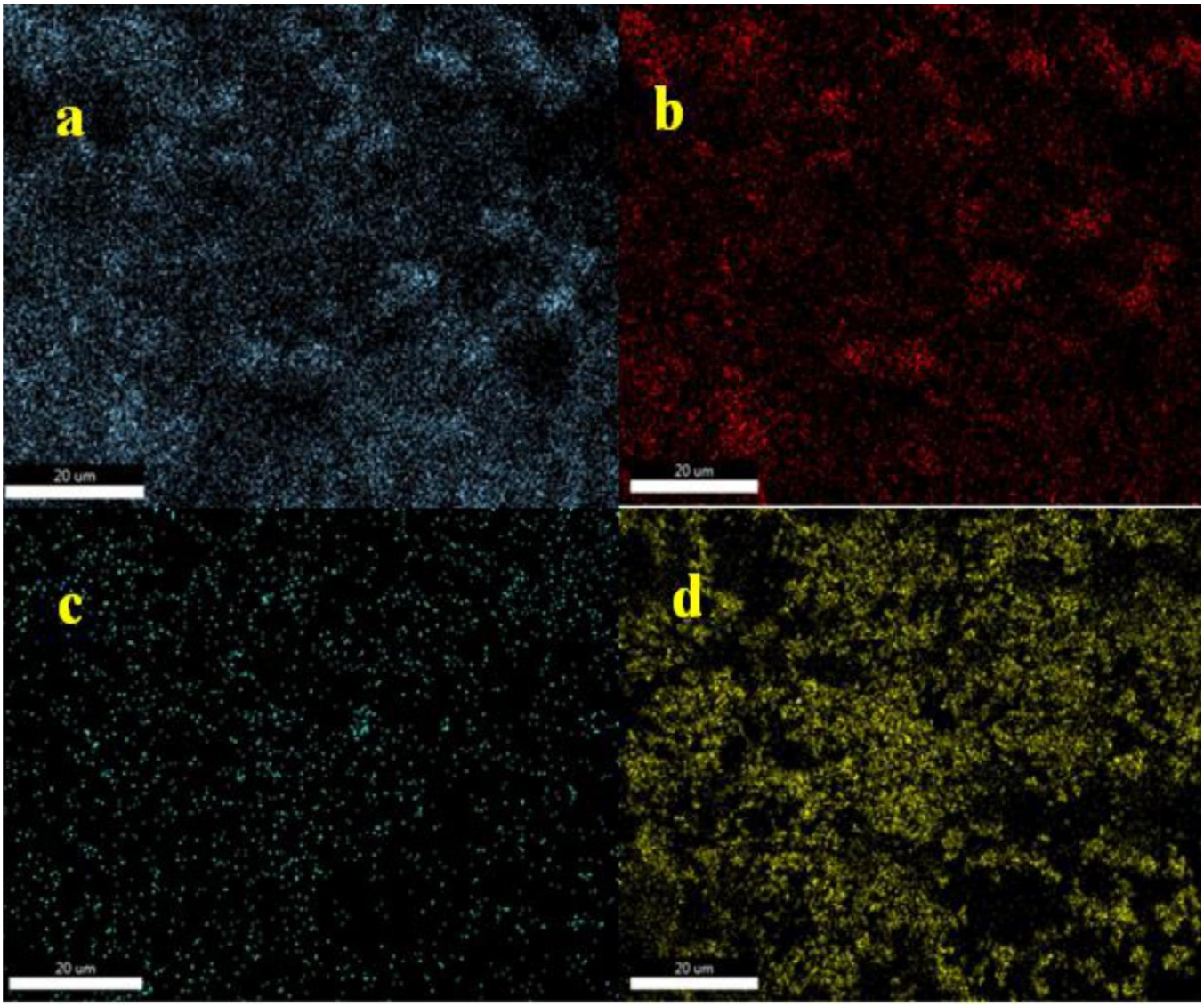


Fig. 4. Colour mapping image of β-CD Ag/Cu nanocomposite

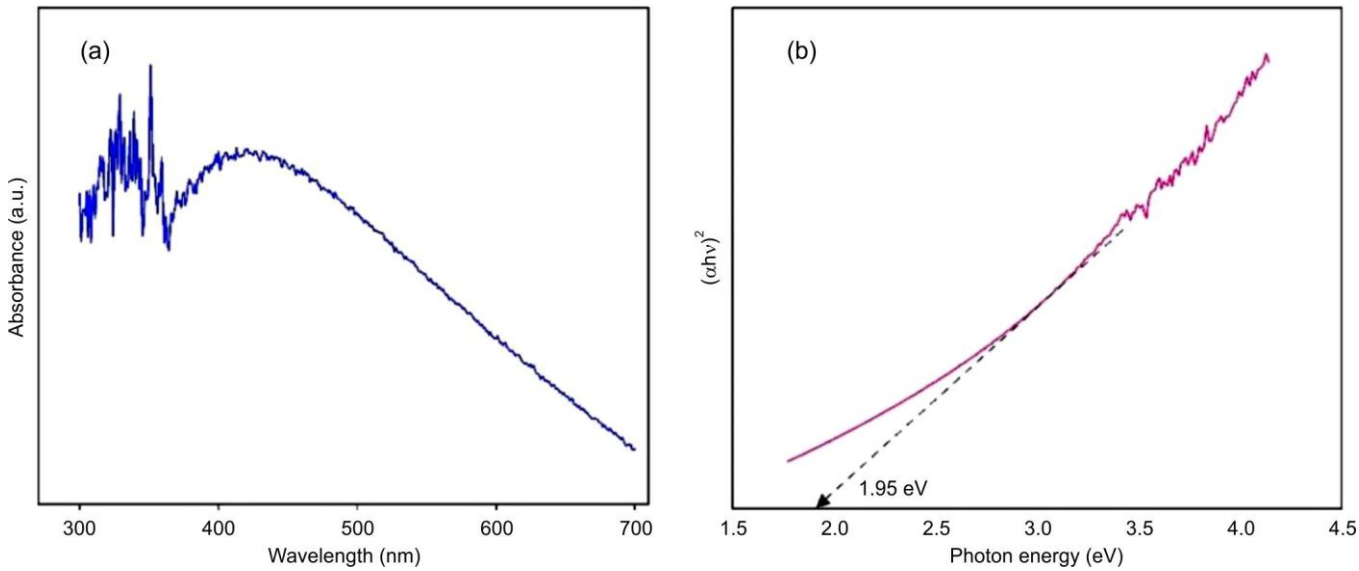


Fig. 5. (a) DRS-UV spectrum and (b) Tauc's plot equation of β-CD Ag/Cu

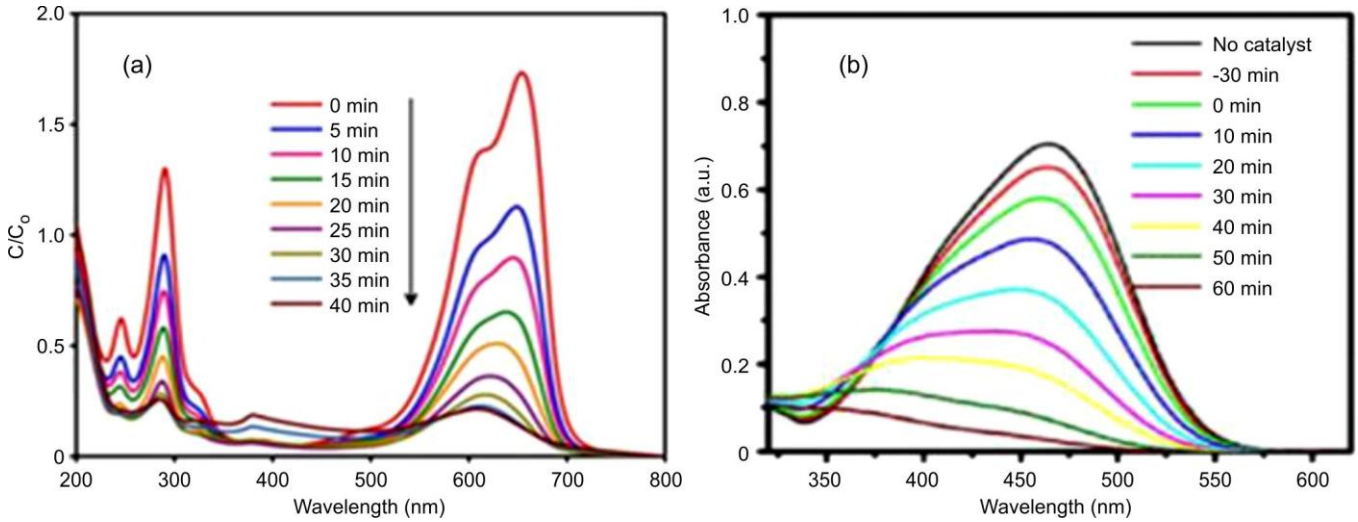


Fig. 6. Absorption spectrum of photodegradation of (a) methylene blue and (b) methyl orange dyes under visible light irradiation

concentration plays a crucial role in achieving efficient photodegradation. As shown in Fig. 7a-b, the photocatalytic degradation of methylene blue (MB) and methyl orange (MO) was investigated using catalyst loadings ranging from 20 to 50 mg. The degradation efficiency increased with catalyst amount up to 40 mg and decreased thereafter due to reduced light penetration and saturation effects caused by excess catalyst. Thus, 40 mg was identified as the optimum catalyst dosage for both MB and MO degradation.

The effect of initial dye concentration on photocatalytic activity was studied by varying MB and MO concentrations from $2 \times 10^{-5}$ to $4 \times 10^{-5}$ M under identical conditions (Fig. 8a-b). The β-CD Ag/Cu nanocomposite achieved maximum degradation efficiencies of 93.13% for MB and 98.65% for MO at $2 \times 10^{-5}$ M. Further increase in dye concentration resulted in reduced degradation efficiency, likely due to the excessive adsorption of dye molecules on the catalyst surface, which limits the availability of active sites.

**Effect of pH:** pH also plays a significant role in the photocatalytic degradation of MB and MO dyes, as wastewater may exhibit acidic or alkaline conditions. The effect of pH was investigated in the range of 5-9 (Fig. 9a-b) using HCl and NaOH to adjust acidic and basic media, respectively. The β-CD Ag/Cu nanocomposite exhibited maximum degradation efficiency for MB at pH 9, whereas MO showed optimum degradation at pH 5. Therefore, pH 9 and pH 5 were identified as the optimal conditions for MB and MO degradation, respectively.

**Kinetics studies:** The kinetics studies of as prepared β-CD Ag/Cu nanocatalyst were studied to identify the rate constant of the degradation reaction. Rate constant values of MB and MO photodegradation reaction were examined by the following equation:

$$\ln\left(\frac{C}{C_o}\right) = -kt \qquad (3)$$

where C is the concentration of solution at a light irradiation time; $C_o$ is the concentration solution before the light irradiation; k is the apparent first-order rate constant; and t is the

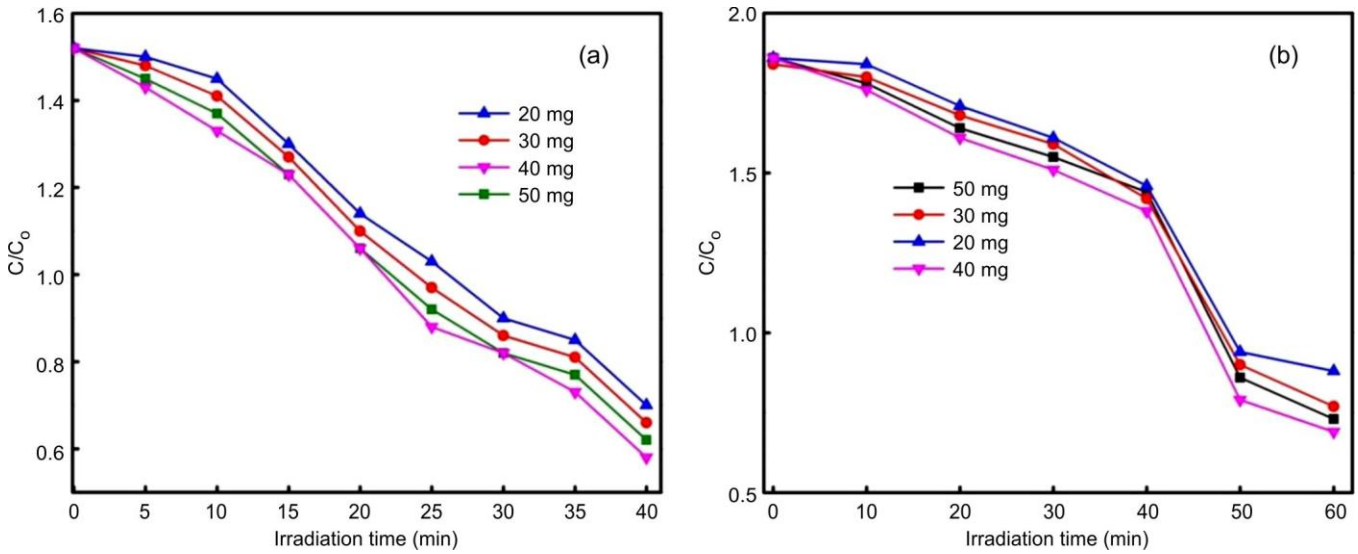


Fig. 7. Different loading dosage of β-CD Ag/Cu in (a) methylene blue and (b) methyl orange dyes

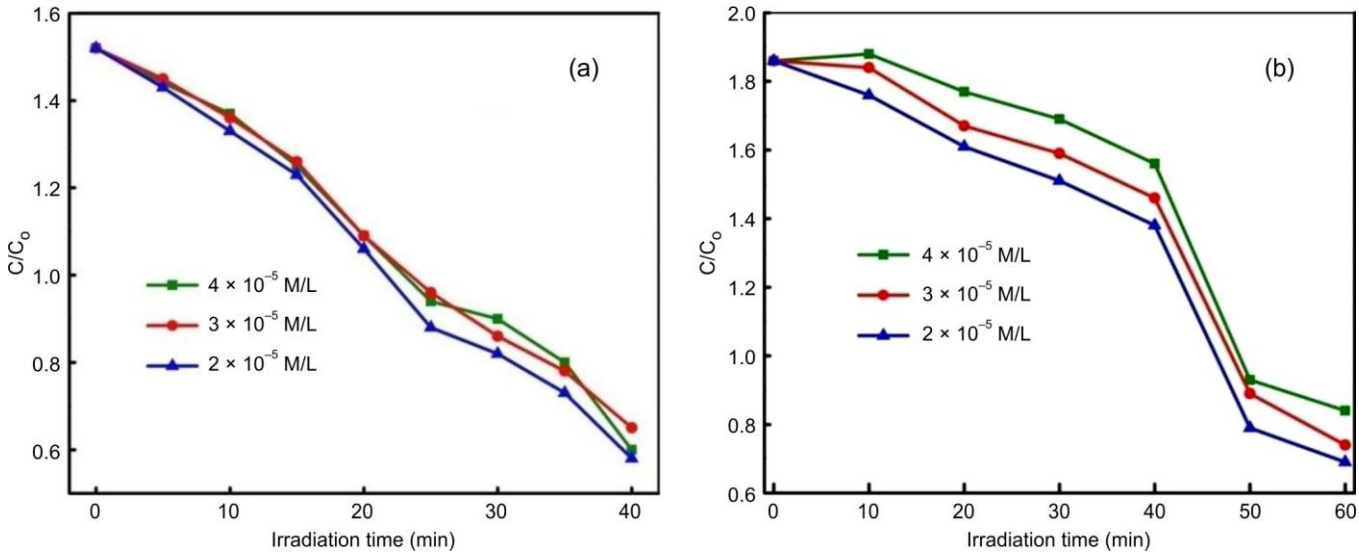


Fig. 8. Different concentration of β-CD Ag/Cu in (a) methylene blue and (b) methyl orange dyes in aqueous solution

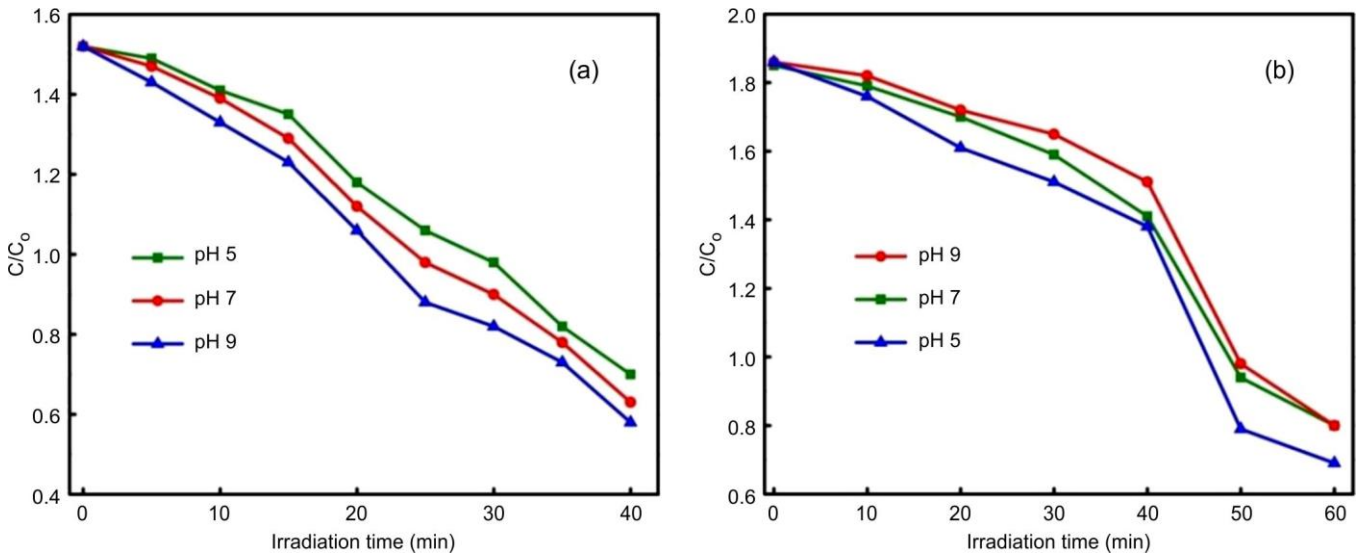


Fig. 9. Different pH of (a) methylene blue and (b) methyl orange dyes in aqueous solution

light irradiation time. β-CD Ag/Cu nanocatalyst shows the rate constant values 0.258 and 0.732 min$^{-1}$, respectively. Fig. 10a-b the β-CD Ag/Cu nanocatalyst exhibits a higher rate constant value compared to without catalyst because of the suitable bandgap value. As a result, the β-CD Ag/Cu nanocomposite exhibits better photocatalytic efficiency to the degradation of MB and MO dyes.

**Antioxidant activity:** Free radicals are known to induce the oxidative stress and contribute to various health disorders. The antioxidant activity of the β-CD Ag/Cu nanocomposite was evaluated using the DPPH radical scavenging assay. The reduction in DPPH absorbance at 517 nm and disappearance of its characteristic violet colour indicate the free radical scavenging ability of the nanocomposite. The β-CD Ag/Cu nanocomposite exhibited concentration-dependent antioxidant activity, with DPPH scavenging efficiencies increasing from 17.53 to 53.16% as the concentration increased from 12.5 to 50 μM (Fig. 11a-b). The observed antioxidant potential may be attributed to electron donation from oxygen-containing functional groups present in the β-CD Ag/Cu nanocomposite [25].

**Antimicrobial activity:** The antibacterial activity of the β-CD Ag/Cu nanocomposite against selected pathogenic bacterial strains is shown in Table-1. The synthesized nanocomposite exhibited effective antibacterial activity against *Enterobacter* sp., *Pseudomonas* sp. and *Klebsiella* sp. Among the tested strains, *Enterobacter* sp. showed the highest sensitivity towards the β-CD Ag/Cu nanocomposite, exhibiting a maximum zone of inhibition (ZOI) of 24 mm. Furthermore, the antibacterial activity was found to increase with increasing concentration of the β-CD Ag/Cu nanocomposite.

## Conclusion

In conclusion, a novel β-CD Ag/Cu nanocomposite was successfully synthesized *via* a facile hydrothermal method and comprehensively characterized using XRD, SEM, EDAX

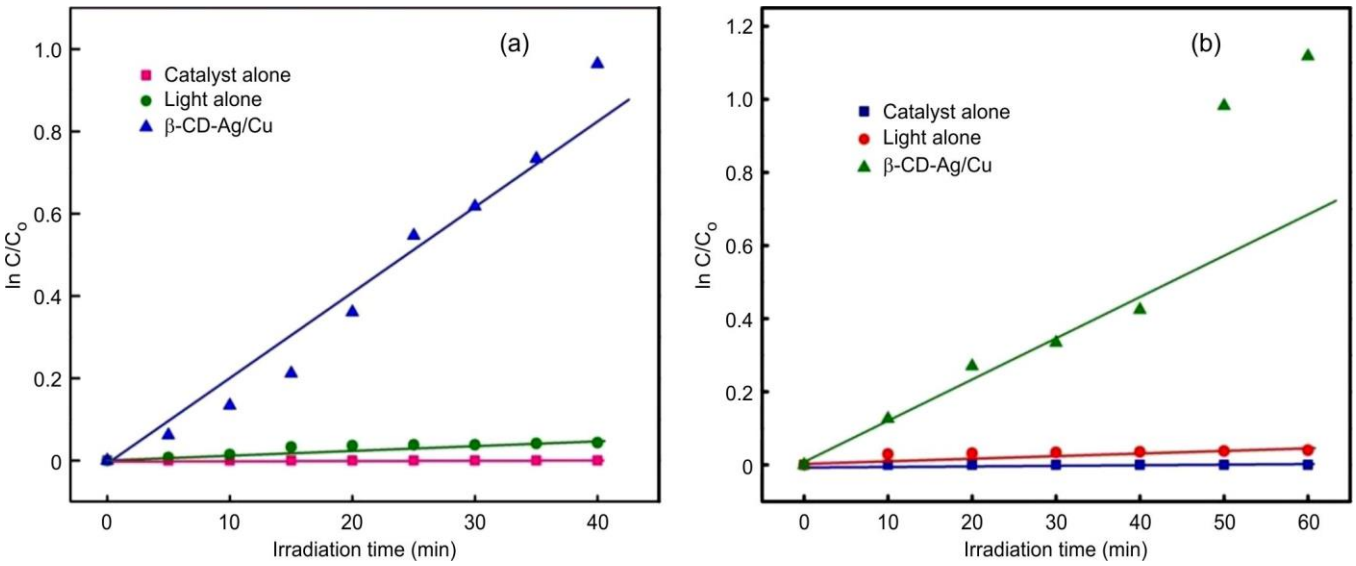


Fig. 10. Kinetics studies of (a) methylene blue and (b) methyl orange dyes degradation with different condition

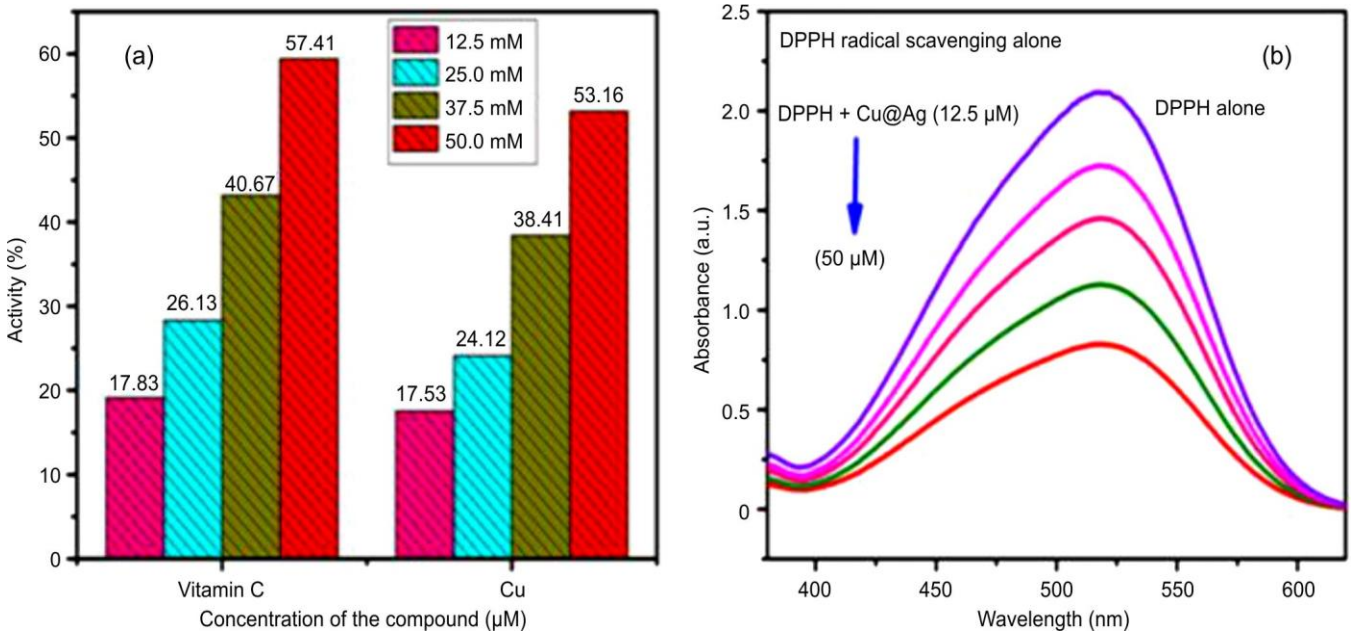


Fig. 11. Antioxidant efficiency of (a) β-CD Ag/Cu nanocomposite and (b) vitamin C against DPPH

TABLE-1
DIAMETER OF ZONES OF INHIBITION (mm) OF SAMPLE β-CD Ag/Cu NANOCOMPOSITE AGAINST MICROORGANISMS

| Microorganism | Nanocomposite concentration (μg/mL) | |
|---|---|---|
| | Control | Test |
| *Enterobacter* sp. | 15 | 24 |
| *Pseudomonas* sp. | – | 23 |
| *Klebsiella* sp. | 16 | 20 |

and DRS-UV techniques. The synthesized nanocomposite exhibited crystalline nature with unique spongy cotton bud-like morphology and an optical band gap of 1.95 eV, enabling efficient visible-light absorption. The β-CD Ag/Cu nanocomposite demonstrated excellent photocatalytic activity towards the degradation of methylene blue (MB) and methyl orange (MO) dyes, achieving degradation efficiencies of 86.20 and 95.71%, respectively, under optimized conditions. The enhanced photocatalytic performance may be attributed to efficient charge separation and suppression of electron-hole recombination. Furthermore, the nanocomposite displayed appreciable antioxidant activity against DPPH radicals and significant antibacterial activity against pathogenic bacterial strains, particularly *Enterobacter* sp. The study highlights the multifunctional potential of β-CD Ag/Cu nanocomposites as efficient photocatalytic, antioxidant and antimicrobial materials.

## CONFLICT OF INTEREST

The authors declare that there is no conflict of interests regarding the publication of this article.

## DECLARATION OF AI-ASSISTED TECHNOLOGIES

During the preparation of this manuscript, the authors used an AI-assisted tool(s) to improve the language. The authors reviewed and edited the content and take full responsibility for the published work.

## REFERENCES


1. P. Yadav, P.K. Surolia and D. Vaya, *Mater. Today Proc.*, **43**, 2949 (2021); https://doi.org/10.1016/j.matpr.2021.01.301
2. C. Lizama, J. Freer, J. Baeza and H.D. Mansilla, *Catal. Today*, **76**, 235 (2002); https://doi.org/10.1016/S0920-5861(02)00222-5
3. M.A. Behnajady, N. Modirshahla and R. Hamzavi, *J. Hazard. Mater.*, **133**, 226 (2006); https://doi.org/10.1016/j.jhazmat.2005.10.022
4. D. Vaya and P.K. Surolia, *Environ. Technol. Innov.*, **20**, 101128 (2020); https://doi.org/10.1016/j.eti.2020.101128
5. R. Saravanan, S. Karthikeyan, V.K. Gupta, G. Sekaran, V. Narayanan and A. Stephen, *Mater. Sci. Eng. C*, **33**, 91 (2013); https://doi.org/10.1016/j.msec.2012.08.011
6. N. Preda, A. Costas, M. Enculescu and I. Enculescu, *Mater. Chem. Phys.*, **240**, 122205 (2020); https://doi.org/10.1016/j.matchemphys.2019.122205
7. C. Shifu, Z. Wei, Z. Sujuan and L. Wei, *Chem. Eng. J.*, **148**, 263 (2009); https://doi.org/10.1016/j.cej.2008.08.039
8. Z.-L. Liu, J.-C. Deng, J.-J. Deng and F.-F. Li, *Mater. Sci. Eng. B*, **150**, 99 (2008); https://doi.org/10.1016/j.mseb.2008.04.002
9. I.A. de Castro, W. Avansi Jr. and C. Ribeiro, *CrystEngComm*, **16**, 1337 (2014); https://doi.org/10.1039/C3CE41668B
10. L. Zhu, M. Hong and G.W. Ho, Scient. Rep., **5**, 11609 (2015); https://doi.org/10.1038/srep11609
11. B. Ma, J. Kim, T. Wang, J. Li, K. Lin, W. Liu and S. Woo, *RSC Adv.*, **5**, 79815 (2015); https://doi.org/10.1039/C5RA15378F
12. T. Sagawa, S. Takeuchi, H. Yoshida, and H. Nakanishi, *J. Phys. Chem. Solids*, **149**, 109762 (2021); https://doi.org/10.1016/j.jpcs.2020.109762
13. A.M. Musuc, *Molecules*, **29**, 5319 (2024); https://doi.org/10.3390/molecules29225319
14. S. Mamman, S.F.F.S. Yacoob, M. Raoov, F.S. Mehamod, N.N.M. Zain and F.B.M. Suah, *J. Anal. Sci. Technol.*, **14**, 3 (2023); https://doi.org/10.1186/s40543-023-00367-4
15. R. Kumar, A. Dhir and V.K. Bhardwaj, *Surf. Interfaces*, **76**, 107937 (2025); https://doi.org/10.1016/j.surfin.2025.107937
16. C. Zheng, W. Zhao, X. Tu and S. Zhou, *Polymers*, **17**, 243 (2025); https://doi.org/10.3390/polym17020243
17. Clinical and Laboratory Standards Institute (CLSI), Abbreviated Identification of Bacteria and Yeast; Approved Guideline, CLSI Document M35-A2, CLSI, Wayne, PA, USA, edn 2 (2008).
18. P.F. Andrade, A.F. de Faria, D.S. da Silva, J.A. Bonacin and M.C. Gonçalves, *Colloids Surf. B Biointerfaces*, **118**, 289 (2014); https://doi.org/10.1016/j.colsurfb.2014.03.032
19. A. Maciollek and H. Ritter, *Beilstein J. Nanotechnol.*, **5**, 380 (2014); https://doi.org/10.3762/bjnano.5.44
20. A. Mani, P. Ramasamy, A.A.M. Prabhu and N. Rajendiran, *J. Mol. Struct.*, **1284**, 135301 (2023); https://doi.org/10.1016/j.molstruc.2023.135301
21. N.C. Horti, M.D. Kamatagi, S.K. Nataraj, M.S. Sannaikar and S.R. Inamdar, *AIP Conf. Proc.*, **2274**, 020002 (2020); https://doi.org/10.1063/5.0022460
22. S.C. Colak, S. Birdogan, E. Aral and G. Kılıc, *Int. J. Hydrogen Energy*, **34**, 5196 (2009); https://doi.org/10.1016/j.ijhydene.2008.10.090
23. I. Saha, A. Ghosh, D. Nandi, K. Gupta, D. Chatterjee and U.C. Ghosh, *Chem. Eng. J.*, **263**, 220 (2015); https://doi.org/10.1016/j.cej.2014.11.039
24. S. Mahalingam, A. Ali, A. Abdulaziz and J. Ramasamy, *Appl. Mater. Interfaces*, **7**, 14905 (2015); https://doi.org/10.1021/acsami.5b02715
25. S. Batool, M. Hasan, M. Dilshad, A. Zafar, T. Tariq, A. Shaheen, R. Iqbal, Z. Ali, T. Munawar, F. Iqbal, S.G. Hassan, X. Shu and G. Caprioli, *Biochem. Syst. Ecol.*, **105**, 104535 (2022); https://doi.org/10.1016/j.bse.2022.104535